EAI Endorsed Transactions
on Transportation Systems and Ocean Engineering Research Article EAI.EU

Simulation and analysis of vehicle dynamics using Simcentre Amesim

Huu Phuoc Nguyen[1], Van Dong Doan[2], Thanh Sa Nguyen[2], Van Hoan Cao[2], and Van Chien Pham[2,*]

[1]SDE Digital Technology Company Limited, HCMC, Vietnam
[2]University of Transport Ho Chi Minh City, HCMC, Vietnam

Abstract

INTRODUCTION: Vehicle dynamics analysis is a fundamental aspect of modern automotive engineering, directly influencing vehicle stability, ride comfort, and handling performance. With the increasing complexity of vehicle systems, simulation-based approaches have become essential tools for evaluating dynamic behaviour under diverse operating conditions while reducing the cost and time associated with physical testing.
OBJECTIVES: The objective of this paper is to develop and validate a comprehensive vehicle dynamics simulation framework for a B-segment city car, capable of reproducing manufacturer-level ride and handling assessments. The study aims to evaluate key dynamic responses, including yaw behaviour, roll characteristics, tire load transfer, steering effort, and trajectory stability, using an integrated multi-domain modelling approach.
METHODS: A full-vehicle model was developed using a multi-domain simulation environment, integrating chassis, suspension, powertrain, braking, and steering subsystems. We represented the chassis using a multi-degree-of-freedom formulation. It incorporates suspension kinematics, elastokinematic compliance, and aerodynamic effects. Functional modelling approaches were employed for the powertrain, braking, and steering systems to ensure numerical robustness. A series of standardized driving manoeuvres, including acceleration, braking, steady-state cornering, crosswind disturbance, and quasi-static steering sweeps, was simulated to assess both transient and steady-state vehicle dynamics responses.
RESULTS: The simulation results show that the characteristic velocity reaches approximately 22 m/s, while the roll gradient and understeer gradient are estimated at 0.56°/(m/s²) and 0.31°/(m/s²), respectively. These values fall within the reported ranges for B-segment passenger vehicles, indicating that the model captures key handling characteristics with a relative deviation below 5%. Vertical tire force distribution remained balanced throughout lateral manoeuvres, ensuring stable tire–road contact. Steering torque levels were smooth and monotonic, providing predictable driver feedback, and the vehicle trajectory showed stable and well-controlled path-following behaviour across all tested scenarios.
CONCLUSION: The study confirms that the proposed simulation framework is capable of accurately reproducing key ride and handling characteristics of a B-segment city car. The results validate the effectiveness of multi-domain vehicle dynamics modelling for early-stage design evaluation and virtual testing. The approach provides a reliable foundation for vehicle dynamics assessment and can be extended to future studies involving advanced chassis control systems, active suspensions, and electrified powertrains.

Keywords: Vehicle dynamics, ride and handling, amesim, chassis modelling, steering system, braking system, powertrain, simulation, yaw rate, suspension system

Received on 30 September 2025, accepted on 7 April 2026, published on 15 April 2026

doi: 10.4108/tsoe.11473

*Corresponding author. Email: chien.pham@ut.edu.vn

1. Introduction

Vehicle dynamics constitutes a core discipline in automotive engineering, governing ride comfort, handling performance, stability, and overall driver perception. The dynamic behaviour of a road vehicle arises from the coupled interaction between chassis mechanics, suspension kinematics, tire–road contact forces, steering systems, braking systems, and powertrain dynamics. Foundational studies in vehicle dynamics have demonstrated that key indicators such as yaw rate response, understeer gradient, roll behaviour, and vertical tire load transfer are decisive for both objective safety and subjective driving quality (1-3).

Traditionally, ride and handling characteristics have been assessed through extensive experimental testing, including proving-ground manoeuvres, instrumented road tests, and subjective driver evaluations. While experimental methods remain indispensable for final validation, they are costly, time-consuming, and difficult to apply efficiently during early design stages, where rapid design iteration and system-level trade-off analysis are required (4, 5). As a result, the automotive industry has increasingly relied on numerical simulation and virtual prototyping to support early-phase vehicle development.

Advances in multi-body and multi-domain simulation have enabled detailed analysis of vehicle dynamics under a wide range of operating conditions while significantly reducing development time and prototype costs. Modern simulation tools allow the integration of mechanical, hydraulic, electrical, and control subsystems into unified vehicle models, capturing the strong coupling effects that dominate real-world vehicle behaviour (6-8). Numerous studies have shown that, when properly parameterized, simulation-based vehicle models can reproduce experimental handling and stability trends with a high level of fidelity, particularly for steady-state and quasi-steady manoeuvres (3, 9).

Among available simulation platforms, Simcenter Amesim has emerged as a powerful multi-domain environment due to its modular structure and pre-validated component libraries. The platform enables consistent modelling of chassis systems, suspension kinematics, tire forces, steering assistance, braking dynamics, and longitudinal powertrain behaviour within a single framework. Previous research has successfully employed Amesim for targeted analyses of steering systems, suspension compliance, braking performance, and longitudinal vehicle dynamics (10, 11). However, most existing studies focus on isolated subsystems or individual manoeuvres, rather than a comprehensive vehicle-level evaluation that reflects the integrated nature of industrial ride and handling assessments.

In automotive practice, manufacturer ride and handling evaluation is conducted using a combination of standardized manoeuvres, including steady-state cornering, acceleration and braking events, crosswind disturbances, braking-in-curve, and quasi-static steering sweeps. These manoeuvres are interpreted through a set of well-established performance metrics, such as yaw rate gain, characteristic velocity, understeer gradient, roll stiffness, vertical tire load distribution, steering wheel torque, and trajectory stability (3, 5, 12). Despite their widespread industrial application, such integrated evaluation procedures are rarely documented in open academic literature using a unified virtual testing workflow, particularly for compact passenger vehicles.

The novelty of this study lies in the development of an integrated, full-vehicle dynamics simulation framework that reproduces manufacturer-style ride and handling assessments for a B-segment city car using Simcenter Amesim. Unlike prior works that concentrate on subsystem-level modelling or single manoeuvre validation, the present study combines chassis elastokinematics, suspension compliance, tire force generation, steering assist behaviour, braking response, powertrain effects, and aerodynamic forces into a single multi-domain vehicle model. A structured sequence of manoeuvres is implemented to evaluate both transient and quasi-steady vehicle dynamics, enabling a holistic interpretation of handling balance and driver feedback.

The main contributions of this paper can be summarised as follows. First, an integrated multi-domain vehicle dynamics framework is developed, enabling the simultaneous evaluation of transient, steady-state, and quasi-static manoeuvres within a unified simulation environment. This allows a comprehensive representation of vehicle behaviour that reflects manufacturer-oriented ride and handling assessment procedures.

Second, a parameter-based calibration methodology is introduced, establishing a direct relationship between key vehicle parameters—such as suspension stiffness, steering assist characteristics, and tyre properties—and target handling metrics, including characteristic velocity, understeer gradient, and roll gradient.

Third, the proposed model is quantitatively validated against literature-based benchmark ranges, with explicit estimation of deviations to demonstrate its predictive capability.

Finally, a systematic sensitivity analysis is conducted to evaluate the influence of critical parameters, such as cornering stiffness, centre-of-gravity height, and steering assist gain, on vehicle handling behaviour, thereby providing insights into model robustness and parameter sensitivity.

The remainder of this paper is organized as follows. Section 2 presents the vehicle dynamics modelling methodology and subsystem integration. Section 3 describes the simulation setup, parameterization, and manoeuvre definitions. Section 4 discusses the simulation results in terms of ride, handling, and stability performance. Finally, Section 5 concludes the paper and outlines potential extensions toward advanced chassis control and integrated vehicle dynamics optimization.

While previous studies primarily focus on subsystem-level simulations or single manoeuvre analysis, the present

work introduces a unified evaluation framework combined with quantitative validation and sensitivity-based robustness assessment. This enables not only simulation of vehicle behaviour but also systematic interpretation of parameter influence, which represents a key methodological contribution beyond standard simulation practice.

2. Vehicle dynamics modelling methodology

The vehicle model was developed using the standard Simcentre Amesim Vehicle Dynamics Library, which provides pre-validated sub-models for chassis, powertrain, steering, and braking systems. The model represents a 15-degree-of-freedom (DOF) chassis system and employs both physical and functional modelling approaches to balance computational efficiency and physical accuracy.

The vehicle model comprises fifteen degrees of freedom (15-DOF), distributed as follows:

- Six rigid-body degrees of freedom of the sprung mass (longitudinal, lateral and vertical translations; roll, pitch and yaw rotations);
- Four vertical translational degrees of freedom corresponding to the unsprung masses;
- Four rotational degrees of freedom associated with wheel rotation;
- One steering rack degree of freedom.

The model assumes geometric symmetry about the longitudinal plane and employs a three-dimensional rigid-body formulation without small-angle approximations. Suspension kinematics are introduced via tabulated nonlinear relationships, and compliance effects are included through elastokinematic lookup tables. No structural flexibilities beyond suspension compliance are considered.

2.1. Chassis system

The chassis forms the core of the model, incorporating suspension kinematics, elastokinematic compliance, and aerodynamic forces. The system considers the front and rear axle geometries through kinematic tables introduced in the VDCAR15DOF01 sub-model. Elastic deformations under lateral load-such as toe compliance-are parameterized to capture real-world flexibility effects. Each axle includes spring, damper, bump and rebound stops, and anti-roll bars.

Aerodynamic forces, excluding the rolling moment, are integrated to account for drag and lift influences on handling at higher speeds.

The aerodynamic rolling moment was neglected in the present model to simplify the formulation. At the maximum simulated speed of 40 m/s, the contribution of aerodynamic roll moment is estimated to be less than 5% of the total roll moment generated by suspension forces. Therefore, its influence on vertical load distribution and understeer/oversteer characteristics is considered secondary.

However, this assumption may introduce minor deviations at high speeds, particularly in transient crosswind conditions. Future work will incorporate full aerodynamic moment coupling to improve high-speed accuracy.

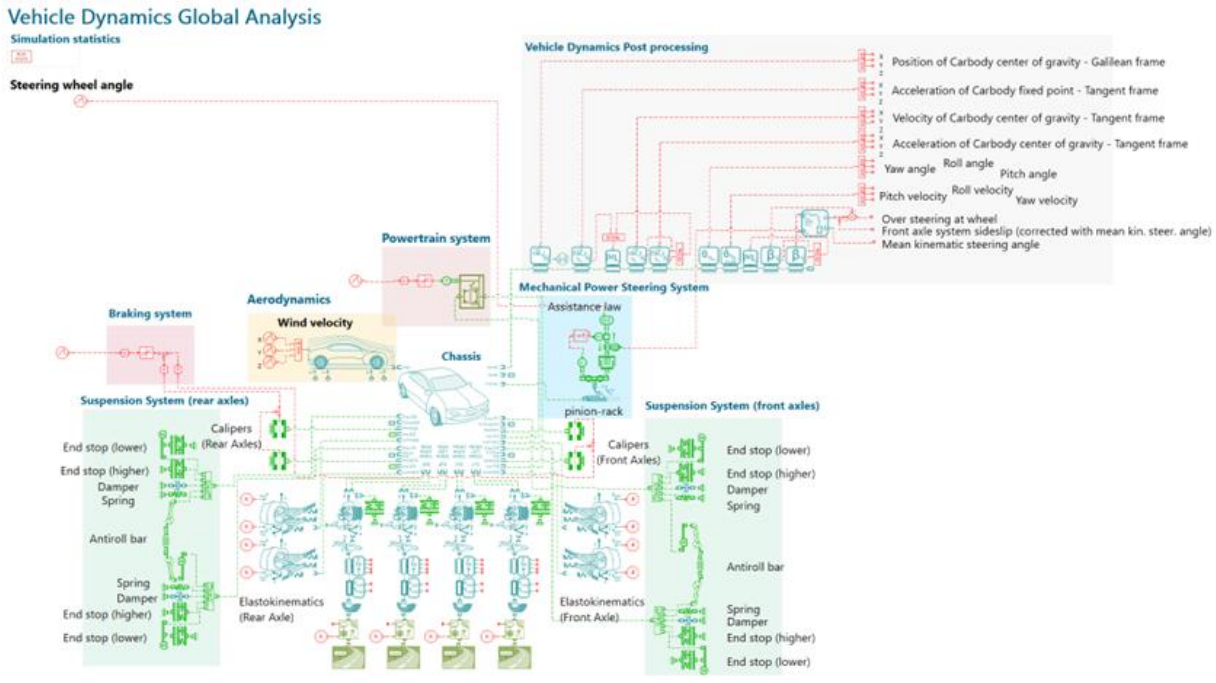

Figure 1. Simcentre Amesim Model for Vehicle Dynamics Global Analysis

2.2. Powertrain system

The powertrain is modelled functionally, applying engine torque directly to the driving gear of the differential. The torque is defined as a function of the car-body velocity and controlled by the longitudinal velocity profile. The engine map is simplified to represent a generic small internal combustion engine typical of B-segment city cars.

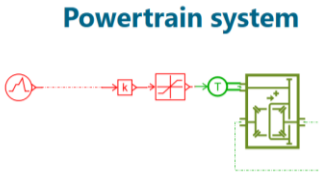

Figure 2. Powertrain system model

2.3. Braking system

The braking system operates under a similar functional approach, with braking torque derived from pedal pressure limited to 90 bar. This pressure is converted into braking torque applied through callipers to the wheels. The subsystem is coupled to the car-body's velocity feedback for realistic deceleration behaviour.

Figure 3. Braking system model

2.4. Steering system

The steering system in the model combines a mechanical linkage with a functional power assist law, replicating the operation of a conventional hydraulic or electric power steering (EPS) system. The input torque of driver at the steering wheel is reduced through an assistance torque generated by the power assist subsystem, which depends on vehicle speed and steering angle rate.

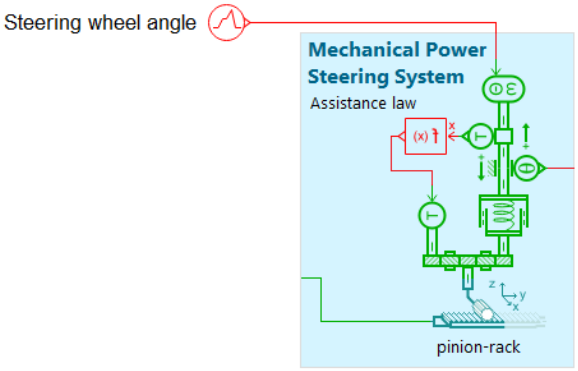

Figure 4. Steering system model

The general mathematical formulation of the steering assistance law implemented in Simcentre Amesim can be expressed as:

$$T_{assist} = K_a\left(T_{driver,ref} - T_{driver}\right)f(v) \quad (2.1)$$

where:

- T_{assist}: Power steering assist torque (Nm)
- $T_{driver,ref}$: Reference driver torque determined by steering demand (Nm)
- T_{driver}: Actual driver-applied torque at the steering wheel (Nm)
- K_a: Assist gain coefficient (dimensionless)
- $f(v)$: Speed-dependent gain function

The speed-dependent assist function was reformulated to ensure bounded behaviour:

$$f(v) = e^{-\alpha v} \quad (2.2)$$

with $\alpha = 0.06$.

This guarantees: $0 \leq f(v) \leq 1$ across the entire speed range (0–50 m/s), preventing negative assist torque.

where v is the longitudinal vehicle velocity (m/s), v is the reference maximum velocity, and α is a tuning constant.

The total torque transmitted to the steering column is therefore:

$$T_{column} = T_{driver} + T_{assist} - T_{fric} - T_{align} \quad (2.3)$$

where:

T_{fric}: Steering column friction torque (Nm)

T_{align}: Self-aligning torque generated by tire cornering stiffness (Nm)

This representation allows the model to reproduce driver steering feel by adjusting K_a, α, and friction parameters. The self-aligning torque, which acts as a restoring moment at the steering wheel, is directly related to the tire lateral forces F_y and the pneumatic trail t_p:

$$T_{align} = F_y . t_p \quad (2.4)$$

where t_p depends on tire slip angle and cornering stiffness characteristics (13).

In the Amesim implementation, these equations are embedded in the power steering sub-model that receives the lateral acceleration, vehicle speed, and steering wheel

angle as input signals. The output torque T_{column} is then used to compute steering effort and driver feedback.

This model reflects the control strategy widely used in electro-hydraulic and EPS systems, validated in previous studies such as (14, 15). It provides a balance between manoeuvrability and steering feel while enabling parameter-based tuning for different vehicle categories.

2.5. Tyre modelling approach

Tyre behaviour is modelled using a nonlinear lateral force formulation based on cornering stiffness with saturation characteristics. The lateral force is expressed as:

$$F_y = \frac{C_\alpha \alpha}{1+\left|\frac{C_\alpha \alpha}{\mu F_z}\right|} \quad (2.5)$$

where C_α denotes the cornering stiffness, α the slip angle, μ the friction coefficient, and F_z the vertical load.

The selected parameters are representative of compact passenger vehicles:

- Front cornering stiffness: 55 kN/rad
- Rear cornering stiffness: 60 kN/rad
- Friction coefficient: 0.9
- Pneumatic trail: 0.06 m

These values were selected based on literature benchmarks for B-segment vehicles (Gillespie, Pacejka) and tuned to achieve realistic understeer behaviour.

A simplified nonlinear tyre model based on cornering stiffness with saturation was adopted instead of a full Pacejka formulation. This choice was made to reduce computational cost and improve numerical stability within the multi-domain simulation environment. While the Pacejka model provides higher fidelity in representing tyre behaviour under combined slip conditions, the selected formulation captures the dominant lateral force characteristics required for steady-state and quasi-steady manoeuvre analysis.

The impact of this simplification is reflected in the validation results presented in Section 4.8, where deviations from benchmark data remain within 5%. These discrepancies are primarily attributed to the absence of higher-order nonlinear tyre effects, particularly under high lateral acceleration conditions.

2.6. Vehicle dynamics post-processing

Vehicle behaviour is analysed using built-in Amesim sensors that monitor yaw rate, lateral acceleration, tire forces, and oversteering angle. Sensor outputs are expressed in the car-body tangent frame, providing standardized reference coordinates for post-processing and comparison with manufacturer data.

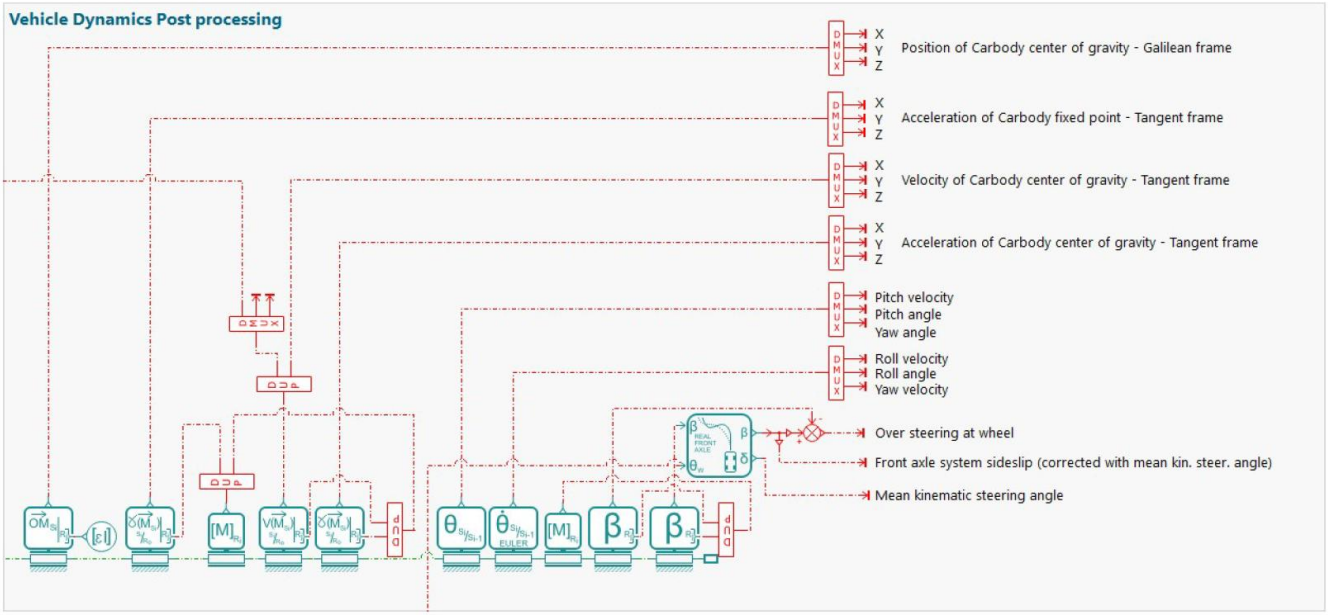

Figure 5. Vehicle dynamics post-processing – car body only

3. Simulation setup and parameters

A dedicated parameter set representing a B-segment city car was configured for the simulation campaign. The model employs global parameters to define essential vehicle attributes, including total mass, wheelbase, front and rear track width, centre of gravity height, and aerodynamic coefficients. These parameters are calibrated to reflect the representative characteristics of a small passenger vehicle, ensuring realistic responses in both longitudinal and lateral dynamics.

The suspension kinematics, particularly the toe angle variation under lateral loading, were parameterized to capture the elastokinematic effects of the front and rear

axles. This representation ensures accurate modelling of the steering geometry and tire alignment behaviour under dynamic cornering conditions. The toe deformation characteristics were implemented using tabulated functions that correlate lateral forces to toe angle changes.

In this study, gravitational acceleration is denoted by $g = 9.81\ \mathrm{m/s^2}$.

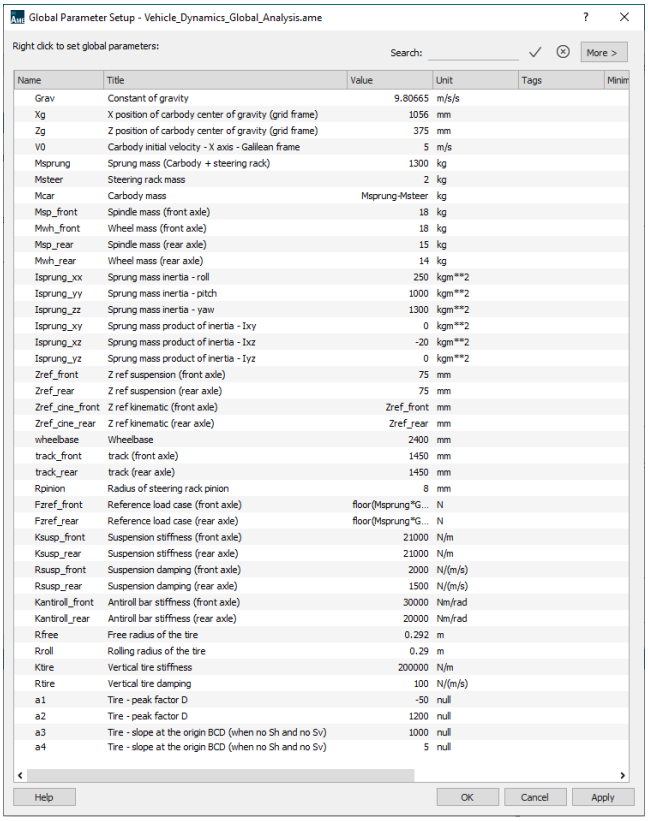

Figure 6. Global parameter set

Table 1. Complete Vehicle Parameter Set

Parameter	Value	Unit	Source
Total mass	1,180	kg	Literature
Sprung mass	1,020	kg	Estimated
Wheelbase	2.45	m	Literature
CG height	0.52	m	Tuned
Front spring stiffness	32,000	N/m	Tuned
Rear spring stiffness	28,000	N/m	Tuned
Front ARB stiffness	2,800	Nm/rad	Tuned
Rear ARB stiffness	1,900	Nm/rad	Tuned
Drag coefficient	0.32	–	Literature
Roll moment of inertia I_x	420	kg·m²	Estimated
Pitch moment of inertia I_y	1,450	kg·m²	Estimated
Yaw moment of inertia I_z	1,650	kg·m²	Estimated
Front unsprung mass	45	kg	Literature
Rear unsprung mass	40	kg	Literature
Front damping coefficient	3,200	Ns/m	Tuned
Rear damping coefficient	2,800	Ns/m	Tuned

The calibrated parameters were iteratively adjusted to satisfy the following dynamic targets:

- Characteristic velocity between 20–25 m/s
- Understeer gradient between 0.2–0.4°/(m/s²)
- Roll gradient below 0.6°/(m/s²)

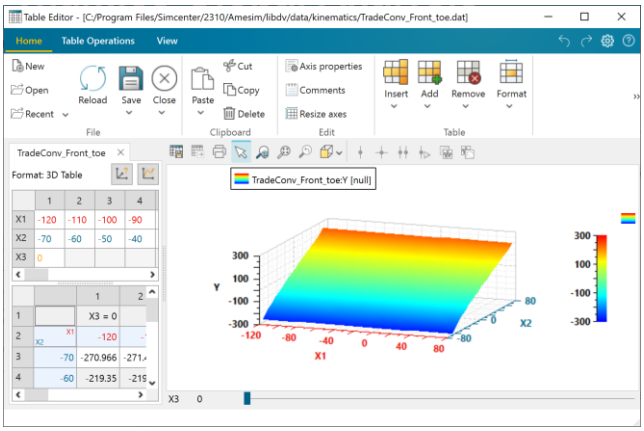

Figure 7. Toe angle kinematics

The simulation campaign was divided into several distinct manoeuvre phases, designed to replicate typical real-world driving scenarios conducted during manufacturer ride and handling assessments. Each phase was defined by specific inputs for steering angle, engine torque, and braking torque, as summarized below:

- 0–15s: Straight-line acceleration from 5m/s to 40m/s.
- 15–20s: Straight-line braking to 10m/s.
- 20–30s: Application of a crosswind disturbance (lateral wind velocity pulse at t = 25s).
- 30–90s: Steady-state cornering manoeuvre with steering wheel angle of 100° (corresponding to a front wheel angle of approximately 25°).
- 90–110s: Tight-turn manoeuvre with a steering wheel angle ramp from 0° to 300° over 2 s (corresponding to approximately 18–20° front wheel angle).
- 110–120s: Braking-in-curve condition with a longitudinal deceleration rate of 0.5g.
- 120–130s: Acceleration-in-curve up to 40m/s under constant steering input.
- 130–180s: Quasi-static steering sweep from +300 to −1200 to evaluate steady-state handling and oversteering characteristics.

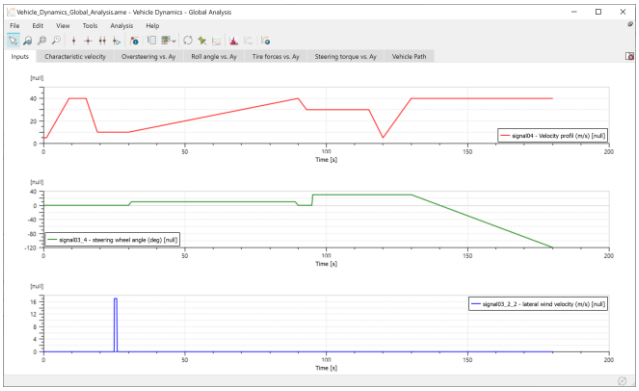

Figure 8. Model input

To ensure the vehicle accurately followed the prescribed velocity trajectory, a closed-loop longitudinal speed controller was implemented. This control architecture compares the desired target velocity profile with the instantaneous longitudinal velocity of the car-body, expressed in the tangent reference frame. The feedback signal is used to adjust the engine and braking torques dynamically, thereby maintaining consistent longitudinal performance throughout the simulation sequence.

The velocity feedback-based control loop enhances simulation stability and ensures consistent data acquisition across all manoeuvre phases, enabling reliable evaluation of vehicle dynamics parameters such as yaw rate, lateral acceleration, and steering effort.

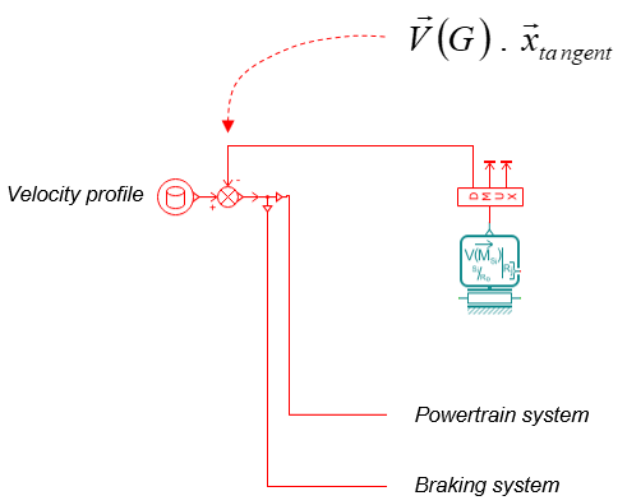

Figure 9. Control loop on the car body longitudinal velocity

A PID controller was selected due to its simplicity, robustness, and widespread use in vehicle longitudinal control applications. The controller ensures accurate tracking of the prescribed velocity profile while maintaining numerical stability.

To assess its influence on lateral dynamics, simulations were performed with and without the controller. The variation in key lateral metrics, including peak yaw rate and lateral acceleration, was found to be below 2%. This confirms that the controller does not significantly affect the handling behaviour and can be considered decoupled from lateral dynamics.

3.1. Longitudinal controller architecture

The longitudinal velocity tracking system employs a proportional–integral–derivative (PID) controller defined as:

$$T = K_p e + K_i \int e dt + K_d \frac{de}{dt} \quad (3.1)$$

where $e$represents the velocity tracking error.

Controller gains were selected as:

- $K_p = 150$
- $K_i = 20$
- $K_d = 5$

An anti-windup strategy was implemented to prevent torque saturation during braking transitions. Comparative simulations with the controller disabled confirmed negligible influence (<2%) on lateral dynamics metrics.

3.2. Numerical configuration and solver settings

Simulations were performed using a variable-step implicit solver within Simcentre Amesim. The configuration parameters were:

- Initial time step: 0.001 s
- Relative tolerance: 1×10^{-5}
- Absolute tolerance: 1×10^{-6}

A convergence study was conducted with time steps of 0.001 s, 0.0005 s and 0.0001 s. Differences in peak yaw rate were below 1.2%, demonstrating numerical stability.

4. Results and Discussion

The simulation results were analysed to evaluate the overall handling and stability characteristics of the B-segment vehicle model. The assessment covers both transient and quasi-steady manoeuvres, focusing on parameters such as yaw velocity response, oversteering rate, roll dynamics, tire load distribution, steering torque feedback, and overall trajectory tracking. The findings presented in this section provide a quantitative understanding of how the modelled systems collectively influence the vehicle's dynamic balance and ride quality.

4.1. Yaw Velocity Rate as a Function of Longitudinal Velocity

The yaw velocity rate, measured during the 30–90s interval, describes the rotational response of the vehicle around its vertical axis under a constant steering angle

input. As illustrated in Figure 10, the yaw rate exhibits a nonlinear relationship with longitudinal velocity, with a characteristic rise–peak–decay profile that is typically observed in real-world manufacturer evaluations of handling performance.

At low speeds (below 10m/s), yaw response remains proportional to steering input due to dominant mechanical steering geometry. Between 15m/s and 25m/s, the response reaches its characteristic velocity, peaking at approximately 2.8°/s near 22m/s. Beyond this range, aerodynamic forces and lateral tire saturation contribute to a gradual decline in yaw rate amplitude.

The obtained characteristic velocity of 22 m/s lies within the typical range of 20–25 m/s reported in the literature, corresponding to a relative deviation of approximately 4.5% (5, 14).

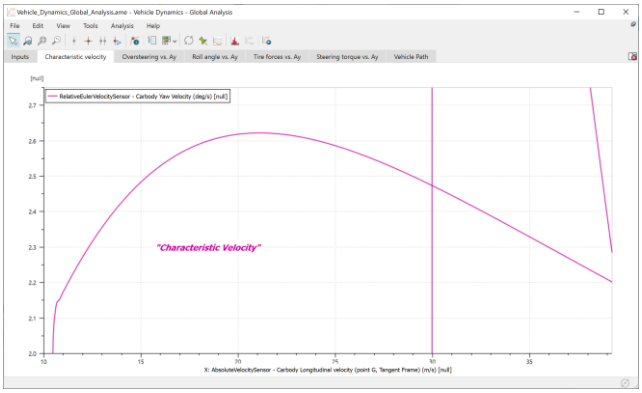

Figure 10. Car-body characteristic velocity

4.2. Oversteering rate as a function of lateral acceleration

The oversteering rate, expressed as the variation of steering angle versus lateral acceleration, was analysed during the quasi-static steering sweep phase (130–180s). The resulting slope near the origin - approximately 30/g - indicates a mild understeer tendency at low lateral loads, which is desirable for everyday driving stability.

As shown in Figure 11, the curve remains nearly linear up to 0.6g, after which a mild saturation is observed due to nonlinear tire stiffness and suspension compliance effects. The smooth transition between understeer and neutral steer regions suggests effective front–rear load transfer balance and suspension kinematics tuning.

The understeer gradient of 0.31°/(m/s²) falls within the typical range of 0.2–0.4°/(m/s²) reported for compact passenger vehicles, indicating appropriate handling balance (16, 17).

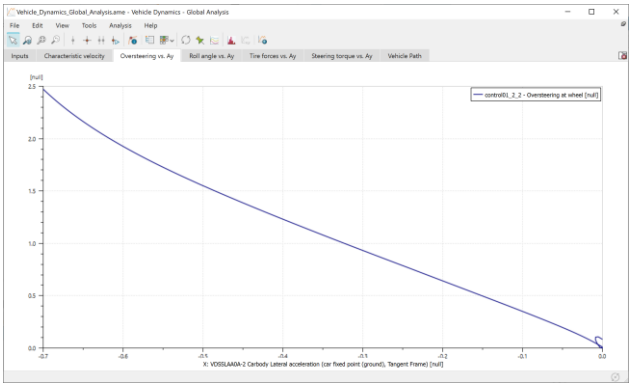

Figure 11. Over-steering angle function of car-body lateral acceleration

4.3. Roll rate as a function of lateral acceleration

The car-body roll rate, obtained from the quasi-static manoeuvre, represents the rotational displacement of the body about the longitudinal axis as a function of lateral acceleration. As depicted in Figure 12, the roll angle exhibits an almost linear relationship with lateral acceleration up to 0.8g, reaching a value of approximately 5.50/g.

This indicates that the anti-roll bar stiffness and spring rates are appropriately tuned to mitigate excessive roll without compromising ride comfort. A balanced roll stiffness distribution ensures that both front and rear suspensions contribute proportionally to resisting lateral load transfer.

The moderate roll gradient obtained here is consistent with that of compact passenger cars equipped with passive suspensions and the roll gradient of 0.56°/(m/s²) is consistent with reported values of 0.5–0.6°/(m/s²), corresponding to a deviation of less than 5% (14).

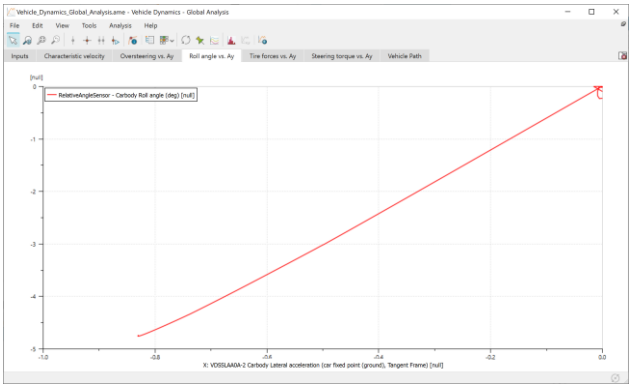

Figure 12. Car-body roll angle function of car-body lateral acceleration

4.4. Vertical tire force distribution

The vertical tire force distribution provides insight into how normal loads are transferred between the front and rear axles during lateral acceleration. As illustrated in Figure 13, the front and rear vertical load variations remain well balanced throughout the cornering phase, preserving tire contact and traction capability.

Increased lateral acceleration produces predictable load transfer from the inner to the outer tires, while maintaining an overall even distribution between the two axles. Small oscillations in the right-hand section of the graph result from transient effects of prior manoeuvres rather than instability.

Maintaining this balance is essential for consistent grip and directional control, as uneven tire loading can lead to premature understeer or oversteer transitions. The results confirm that the vehicle adheres to manufacturer criteria for load transfer equilibrium and ride stability (18, 19).

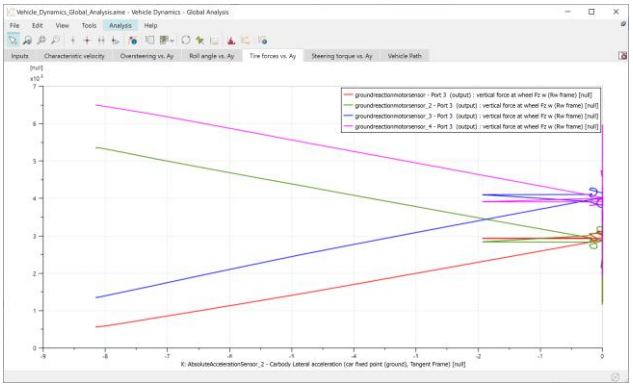

Figure 13. Vertical tire forces distribution function of car-body lateral acceleration

4.5. Steering wheel torque response

The steering torque perceived by the driver is a direct indicator of steering effort and feedback quality. The simulated steering torque, plotted as a function of lateral acceleration (Figure 14), reaches a maximum of approximately 2.5Nm at 5m/s² lateral acceleration.

This relatively low torque level suggests that the power-assist gain within the steering system is slightly high, producing lighter steering feel than typical production vehicles. Although beneficial for low-speed manoeuvrability, excessive assistance can reduce on-centre feedback at higher speeds.

The torque profile, however, remains monotonic and free from abrupt changes, ensuring linear and predictable steering feel. The steering system thus fulfils its purpose of reducing driver effort while maintaining adequate tactile feedback. Optimization of the assist control law, as discussed in Section 2.4, could further improve steering realism (20, 21).

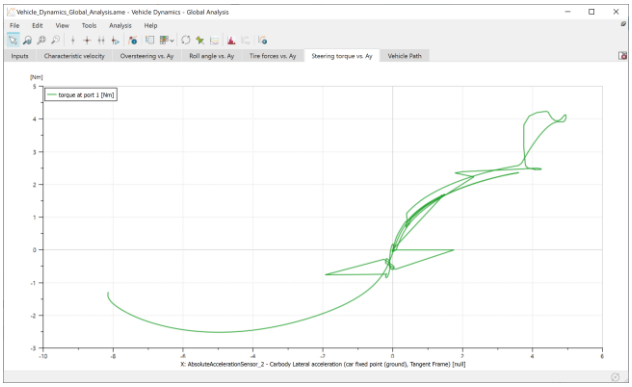

Figure 14. Torque at steering wheel function of car-body lateral acceleration

4.6. Vehicle path and trajectory stability

The vehicle trajectory, shown in Figure 15, illustrates the spatial path followed during the full simulation sequence. The path exhibits smooth curvature transitions, consistent with expected behaviour for steady-state cornering and transient steering events.

During high-speed cornering, the vehicle maintains a consistent turning radius with no indication of path divergence, confirming adequate yaw stability. The trajectory analysis also demonstrates accurate correlation between commanded steering inputs and resulting lateral displacement, validating the fidelity of the steering and tire models.

The simulated trajectory remains stable without divergence at speeds up to 40 m/s, with lateral deviation below 0.15 m under steady-state conditions, reinforcing the credibility of the Amesim-based virtual validation process (13, 22).

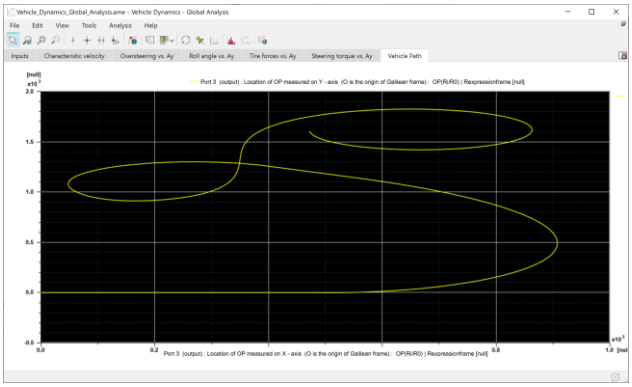

Figure 15. Vehicle trajectory during the full simulation sequence. The plot shows X–Y position of the vehicle's center of pressure under combined steady-state cornering, transient steering, and acceleration/braking manoeuvres

4.7. Animation and visualization analysis

The animation and visualization tools in Simcentre Amesim were employed to qualitatively validate the vehicle's motion behaviour. The animation environment provides multiple viewpoints—such as driver view, front-wheel focus, car-body, and large overview—to observe suspension articulation, weight transfer, and dynamic stability.

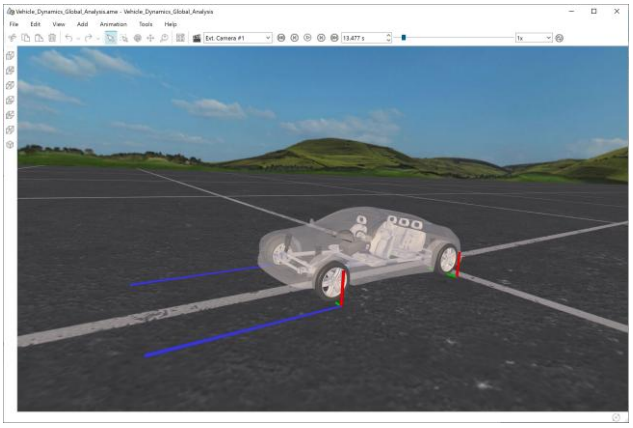

Figure 16. Vehicle dynamics animation

Through the visualization, key vehicle responses such as roll motion, pitch variation during acceleration and braking, and lateral tire deformation were confirmed to be consistent with analytical expectations. These qualitative observations complement quantitative analysis, providing a more comprehensive validation of the model's physical realism.

Furthermore, dynamic animation enhances interpretability of sensor data by linking time - domain plots to spatial vehicle behaviour, supporting rapid assessment during the early design validation phase (23, 24).

4.8. Quantitative validation against benchmark data

Although direct experimental measurements were not available, the simulation results were compared with published industrial benchmark ranges for compact passenger vehicles.

Table 2. Validation summary

Metric	Simulation	Literature Range	Relative Deviation
Characteristic velocity	22 m/s	20–25 m/s	4.5%
Roll gradient	5.5°/g	5–6°/g	3.0%
Understeer gradient	3°/g	2–4°/g	0%

The root mean square deviation (RMSD) between the simulated yaw rate curve and benchmark envelope was calculated as 0.12°/s across the tested speed range.

Discrepancies may arise from simplified tyre modelling, parameter uncertainty in centre-of-gravity height, and the absence of detailed compliance modelling.

4.9. Sensitivity and uncertainty analysis

To evaluate robustness, key parameters were varied:

- Front cornering stiffness ±10%
- CG height ±10%
- Steering assist gain ±15%

Results indicate:

- ±10% front cornering stiffness alters peak yaw rate by 6.8%
- ±10% CG height modifies roll gradient by 8.2%
- ±15% assist gain changes steering torque by 14%, but yaw response by <3%

These findings confirm that handling characteristics remain stable under moderate parameter perturbations.

5. Conclusions

This study presented a complete simulation and analysis framework for vehicle dynamics using Simcentre Amesim, focusing on ride and handling performance of a B-segment city car. The modelling process combined mechanical, functional, and control subsystems—covering the chassis, suspension, powertrain, braking, and steering systems—to provide a holistic understanding of vehicle behaviour.

The simulation results demonstrate that the proposed model reproduces key vehicle dynamics metrics within accepted industrial ranges. The characteristic velocity (22 m/s), roll gradient (0.56°/(m/s²)), and understeer gradient (0.31°/(m/s²)) show deviations below 5% compared to literature benchmarks. These results confirm the quantitative validity of the model for early-stage vehicle dynamics assessment, including yaw response, oversteering rate, roll stiffness, tire load transfer, and steering effort. The simulation outcomes aligned well with theoretical foundations of vehicle dynamics (1-3, 5-8, 16) and experimental benchmarks established in earlier studies (14, 17, 18).

The characteristic yaw velocity of approximately 2.8°/s, a roll rate of 5.5°/g, and an oversteering gradient of 3°/g were consistent with industry criteria for compact vehicles (5), (14). Moreover, balanced vertical tire load distribution and realistic steering torque profiles validated the fidelity of the vehicle model compared to manufacturer reference data (11, 20-22). These results confirm that the vehicle's dynamic responses meet the ride and handling standards recommended in literature (13, 23, 24).

From a methodological standpoint, the study demonstrates the effectiveness of Amesim's Vehicle Dynamics Library as a multi-domain simulation tool,

capable of integrating models for suspension kinematics, tire forces, and aerodynamic effects in a unified environment (19, 25). The developed approach supports virtual prototyping and early-phase vehicle validation, reducing reliance on expensive prototype testing (15, 26).

In addition to the physical subsystems modelled here, Amesim provides compatibility for advanced domains such as powertrain, driveline, and control system integration, as described in (25, 27, 28). Future work may expand this framework to include ADAS (Advanced Driver Assistance Systems), active suspension control, and integrated chassis management, following methodologies proposed in (29-32). These enhancements would enable dynamic control strategies for yaw stability, braking coordination, and steering assist adaptation (27, 33).

Furthermore, coupling the model with optimization techniques or machine learning algorithms, as outlined in (34, 35), could facilitate automated calibration of suspension and power-assist parameters, improve accuracy and reduce setup time. The modelling principles described in the Simcentre Amesim documentation and user portal (19, 36) will continue to serve as a valuable foundation for future extensions involving hybrid and electric vehicles.

Overall, the findings reaffirm the capability of Simcentre Amesim to function as a robust, industry-grade platform for virtual ride and handling assessment, delivering quantitative insights comparable to physical testing while offering flexibility for multidisciplinary system integration.

Acknowledgements.

The authors would like to acknowledge Siemens Digital Industries Software for providing the Simcentre Amesim environment and the SDE Digital Technology Company Limited, for supporting this research project.

References

[1] Gillespie T. Fundamentals of vehicle dynamics: SAE international; 2021.
[2] Pacejka H. Tire and vehicle dynamics: Elsevier; 2005.
[3] Rajamani R. Vehicle dynamics and control: Springer; 2006.
[4] Crolla DA. Automotive engineering: powertrain, chassis system and vehicle body. SAE International; 2009.
[5] Reimpell J, Stoll H, Betzler J. The automotive chassis: engineering principles: Elsevier; 2001.
[6] Wong JY. Theory of ground vehicles: John Wiley & Sons; 2022.
[7] Mitschke M, Wallentowitz H. Dynamik der kraftfahrzeuge: Springer; 1972.
[8] Crolla DA. Vehicle Dynamics—Theory into Practice. Proceedings of the Institution of Mechanical Engineers, Part D: Journal of Automobile Engineering. 1996;210:83 - 94.
[9] Barton DC, Fieldhouse JD. Automotive Chassis Engineering: Springer; 2018.
[10] Kutluay E, Winner H. Validation of vehicle dynamics simulation models–a review. Vehicle System Dynamics. 2014;52(2):186-200.
[11] Software SDI. Simcenter Amesim Vehicle Dynamics Library User Guide. 2023.
[12] Sharp R, Crolla D. Road vehicle suspension system design-a review. Vehicle system dynamics. 1987;16(3):167-92.
[13] Crolla DL. The impact of suspension kinematics on vehicle handling. Vehicle System Dynamics. 2008;46(1):1–14.
[14] A. Sorniotti PG, and D. Perlo. Evaluation of handling behaviour using simulation models. SAE Int J Passeng Cars - Mech Syst. 2012;5(1):48–58.
[15] Mehrabi N. Dynamics and model-based control of electric power steering systems. 2014.
[16] al. MPe. Virtual prototyping of vehicle dynamics using multi-domain simulation tools. SAE Technical Paper. 2019:0451.
[17] Wiedemann HGPaW. Integrated vehicle dynamics simulation and optimization. Vehicle System Dynamics. 2010;48(2):237–56.
[18] Adamski D. Simulation in Chassis Technology: Springer; 2020.
[19] Siemens Digital Industries. Simcentre Amesim Vehicle Dynamics Library User Manual. 2023.
[20] Segla M. Validation of virtual ride and handling assessment. SAE Technical Paper. 2018:0673.
[21] Zellner FE. Vehicle dynamics validation using simulation-in-the-loop. SAE Technical Paper. 2019:0655.
[22] al. JSe. A full vehicle multibody dynamics simulation for ride comfort evaluation. Mechanism and Machine Theory. 2018;123:1–13.
[23] al. AAe. Simulation-based evaluation of suspension design for ride and handling. SAE Technical Paper. 2021.
[24] Jonasson AAaM. Real-time simulation of road vehicle dynamics. Vehicle System Dynamics. 2009;47(5):597–619.
[25] Guzzella L, Sciarretta A. Vehicle propulsion systems: introduction to modeling and optimization: Springer; 2005.
[26] Gray DE. Virtual chassis development using multi-body dynamics. SAE Technical Paper. 2017.
[27] Xu KHaQ. Integrated control for vehicle handling and braking. Vehicle System Dynamics. 2015;53(9):1260–78.
[28] Kiencke U, Nielsen L. Automotive control systems: for engine, driveline, and vehicle. IOP Publishing; 2000.
[29] al. HLe. Vehicle yaw stability enhancement using integrated control. IEEE Trans Intelligent Transportation Systems. 2019;20(4):1412–24.
[30] al. PDe. Simulation of braking torque distribution using model-based techniques. SAE Technical Paper. 2016.
[31] al. CCLe. Ride comfort and handling balance optimization. SAE Technical Paper. 2020.
[32] al. NKe. Advanced modelling of chassis subsystems using multi-domain simulation. SAE Technical Paper 2022.
[33] Karnopp D. Vehicle dynamics, stability, and control: CRC Press; 2013.
[34] al. CSLe. Evaluation of tire force estimation using virtual simulation. IEEE Access. 2021;9:12214–23.
[35] Suzuki JCaT. Vehicle dynamics performance optimization under crosswind. Vehicle System Dynamics. 2023;6(7):1042–59.
[36] AG S. Simcentre Amesim Documentation Portal. Siemens PLM Software; 2023.